A PETROLOGICAL MODEL FOR THE ORIGIN OF MARTIAN SHERGOTTITE MAGMAS BASED ON THEIR MAJOR ELEMENT, TRACE ELEMENT, AND ISOTOPIC COMPOSITIONS

L. E. Borg[1] and D. S. Draper[1], [1]Institute of Meteoritics University of New Mexico, Albuquerque, NM 87131 USA

Introduction: Defining the mineralogy and composition of martian mantle source regions has proved to be a difficult task because: (1) the martian sample set does not include samples of the mantle, and (2) many of the samples are either cumulates or are highly fractionated and therefore not in equilibrium with the mantle. Despite these complexities, isotopic evidence suggests that Mars had a magma ocean that crystallized at ~4.53 Ga, and that melting of magma ocean cumulates between ~175-575 Ma produced the shergottite parental magmas [e.g., 1-3]. This scenario has permitted the Rb/Sr, Sm/Nd, and Lu/Hf ratios of the martian magma sources to be estimated from their initial Sr, Nd, and Hf isotopic compositions [4]. Below we estimate the relative abundances of additional incompatible elements in the magma source regions using a magma ocean crystallization model.

Approach: The models presented below follow the approach used by Snyder et al. [5] to estimate the composition of lunar magma source regions. First, the mineralogy of the martian magma ocean cumulates is estimated from the results of high pressure experiments. Next, a combination of equilibrium and fractional melt models is used to estimate the major and trace element abundances in the various cumulate packages. Finally, the mineralogy of depleted martian mantle (DMM) is estimated by determining which combination of cumulates: (1) yield melts with major element compositions that match those of the most mafic parental magma [Am; ALH77005; 6], and (2) have the Rb/Sr, Sm/Nd, and Lu/Hf ratios of the most incompatible element depleted martian meteorite (QUE94201) source region.

Experimental constraints on the source regions: We chose Homestead L5 ordinary chondrite as an analog for early martian mantle immediately following core formation, i.e. as the bulk composition of an early martian magma ocean. This composition was used in the partitioning and phase equilibrium experiments of Draper and coworkers [7-8]. These results, as well as those of Agee et al. [9] and Ohtani et al. [10], were used to infer a magma ocean crystallization sequence.

We investigated several crystallization sequences to generate magma ocean cumulate packages. These ranged from those having olivine and pyropic garnet as near-liquidus phases (representing lower-P conditions) to those having majoritic garnet on, or near, the liquidus (representing higher P). In each step of a given sequence, we calculated progressive melt compositions using equilibrium and fractional (at melt fractions <20%) crystallization models and the appropriate mineral assemblage. Coexisting solid bulk compositions were calculated by mass balance. Each sequence yielded four or five separate cumulate packages after 98% crystallization of the starting magma ocean composition. We then calculated 10% partial melts of each of these packages for comparison with Am and other proposed martian parental melts.

Fig. 1 compares calculated melts from the various sequences to the estimated parental melts. The crystallization sequence that yields partial melts that are the best match to Am [blue line Fig. 1] consists of these five steps: (1) Crystallization of majorite until 5 percent solid (PCS); (2) olivine + majorite (80:20) to 20 PCS; (3) olivine + orthopyroxene (50:50) to 60 PCS; (4) orthopyroxene + clinopyroxene (60:40) to 90 PCS; (5) clinopyroxene + ilmenite (90:10) to 98 PCS.

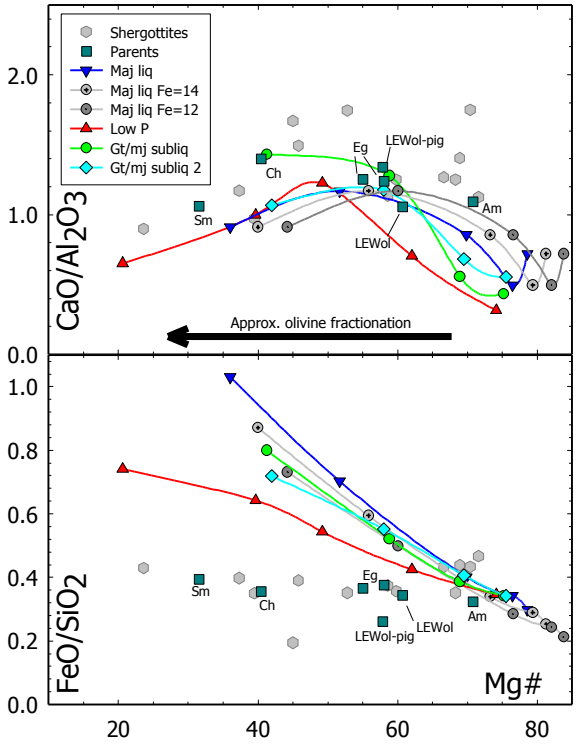

Fig. 1. 10% melts of cumulate packages produced in crystallization sequences. *Maj liq* = liquidus majorite. *Gt/mj subliq* = mildly majoritic garnet in subliquidus. Most parental melts are not primitive and lie off the melting trends.

There are several observations from this modeling including: (1) these processes reproduce the composition the most primitive parent (Am) well, (2) majoritic garnet must crystallize early to produce the superchondritic CaO/Al_2O_3 of martian parents, and (3) the strongest mismatch between the models and the parent compositions is with respect to Fe. Model melts are more

Fe-rich than the parental compositions. This mismatch could be alleviated if the martian mantle were less Fe-rich (gray curves on Fig. 1 show results for a martian mantle with 14 and 12 wt% FeO) or by increasing fO_2 during subsequent differentiation.

Trace element and isotopic constraints on the source regions: The trace element compositions of the various cumulates are calculated using the crystallization sequence discussed above and the bulk composition of silicate Mars of [11]. The Rb abundance of bulk Mars was lowered from 3.5 to 1.5 ppm so that the bulk Mars $^{87}Rb/^{86}Sr$ ratio is 0.32, a maximum value based on Rb-Sr isotopic analysis of martian meteorites [12]. Partition coefficients for olivine and pyroxenes are summarized in [1], whereas the coefficients for garnet are from [1] and the 7 GPa experiments of [7].

The initial Sr, Nd, and Hf isotopic compositions of QUE indicate that it is derived from a source region with $^{87}Rb/^{86}Sr$, $^{147}Sm/^{144}Nd$, and $^{176}Lu/^{177}Hf$ ratios of 0.037, 0.287, and 0.048 respectively [3, 13]. These ratios are very similar to the ratios calculated for the fourth PCS step, as well as the weighted average of the cumulates modeled in PCS steps 2-4 ($^{87}Rb/^{86}Sr$ = 0.031; $^{147}Sm/^{144}Nd$ = 0.303; $^{176}Lu/^{177}Hf$ = 0.050). This fact, combined with the observation that partial melts of a combination of these cumulates yield major element abundances and ratios similar to the most primitive martian parental magmas, indicate that the average PCS 2-4 cumulate package is the most representative of the QUE source, and thus DMM.

The results of the trace element models are presented in Fig. 2a. This is a plot of the chondrite-normalized-trace-element abundances of the various cumulates. The shaded area represents the boundary between the two cumulate packages that have Rb/Sr, Sm/Nd, and Lu/Hf ratios that are most similar to the QUE source. Note that these sources are depleted in the most incompatible elements, a feature that is consistent with the LREE-depleted pattern of QUE.

Fig. 2b is a plot of the DMM-normalized-trace-element abundances of the whole rock compositions of the shergottites with the most mantle-like Sr and Nd isotopic compositions (i.e., QUE, DaG476, SaU005, and Dhofar 019). The composition of QUE (Mg# = 38) plots substantially above the other meteorites (Mg# 63-71) primarily because it has undergone substantially more fractional crystallization. As a result, to better represent the composition of the unfractionated QUE parent, the QUE whole rock pattern is visually transposed onto the whole rock patterns of the other meteorites in Fig. 2b. From this figure it is apparent that many incompatible elements, including Rb, U, K, Sr, and the MREE have ~10x DMM abundances consistent with

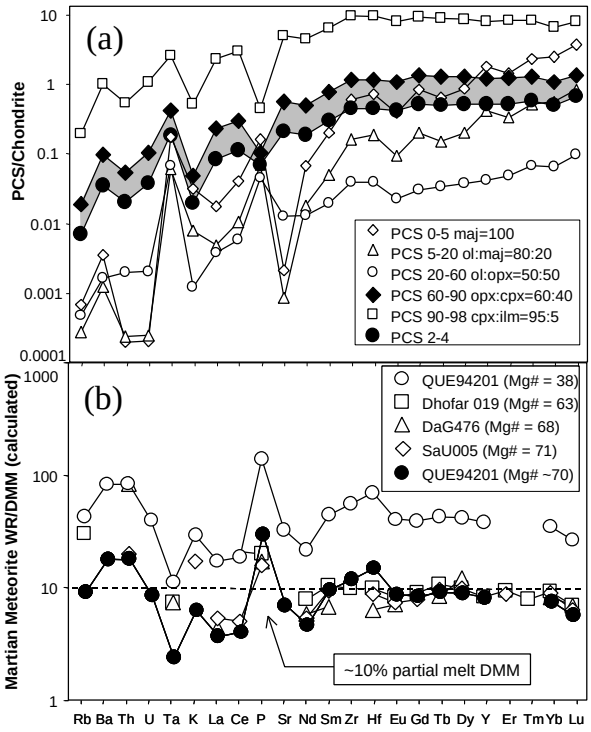

Fig. 2. Trace element abundances of (a) PCS steps and (b) bulk martian meteorites. Dashed line is ~10% melt of DMM

~10% partial melting of DMM. Other elements, however, are significantly above (Ba, Th, P, Zr, and Hf) or significantly below (La, Ce, Nd, Yb, and Lu) the ~10% partial melt line (dashed) on Fig. 2b. Some of these variations can potentially be explained by imprecise data (e.g., Ba and possibly Th and Ta). Low abundances of HREE in the martian whole rocks relative to their calculated sources most likely reflects the presence of garnet in their source regions during melting [3, 13]. Low abundances of LREE seem to require that the LREE behave more compatibly than is predicted by magma ocean crystallization models using olivine, pyroxene, and garnet. The higher abundances of high field strength elements, P, Zr, and Hf, seems to require the addition of another component that has not been considered in the models as suggested by [13].

References: [1] Shih et al. (1982) *GCA* **46,** 2323-2344. [2] Harper et al. (1995) *Nature* 267, 213-7. [3] Borg et al. (1997) *GCA* 61, 4915-4932. [4] Borg (2002) Workshop: Unmixing the SNCs. LPI contrib. #1134, 9-10. [5] Snyder et al. (1992) *GCA* **56,** 3809-3823. [6] McSween et al. (1988) *LPSC* **XIX,** 766-767. [7] Draper et al. (in review) *PEPI.* [8] Wasserman et al. (2001) *LPSC* **XXXII**, 2029. [9] Agee et al. (1995) *JGR* **100,** 17,725-17,740. [10] Ohtani et al. (1989) *CMP* **103,** 263-269. [11] Lodders & Fegley (1997) *Icarus* **126,** 373-394. [12] Borg et al. (in press) *GCA.* [13] Blichert-Toft et al. (1999) *EPSL* **173,** 25-39.